Acta Materialia 143 (2018) 77-87

Contents lists available at ScienceDirect

Acta Materialia

journal homepage: www.elsevier.com/locate/actamat



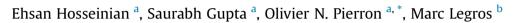
### Full length article

# Size effects on intergranular crack growth mechanisms in ultrathin nanocrystalline gold free-standing films



CrossMark

Acta materialia



<sup>a</sup> G.W. Woodruff School of Mechanical Engineering, Georgia Institute of Technology, Atlanta, GA, 30332-0405, USA
<sup>b</sup> CEMES-CNRS, 29 Rue Jeanne-Marvig, 31055 Toulouse, France

#### ARTICLE INFO

Article history: Received 19 July 2017 Received in revised form 29 September 2017 Accepted 1 October 2017 Available online 3 October 2017

Keywords: Crack growth In situ TEM Nanocrystalline films

#### ABSTRACT

This study investigated the combined effects of thickness (30 vs 100 nm) and average grain size (40 vs 70 nm for the thicker films) on the crack propagation mechanisms in ultrathin nanocrystalline gold microbeams, using a microelectromechanical system device to perform in situ transmission electron microscope (TEM) tensile experiments. Monotonic tensile tests of the two types of microbeams show similar strength levels (~400 MPa) and ductility (~2%). However, the thicker specimens exhibit a much more ductile behavior under repeated stress relaxation experiments, which the in situ TEM experiments revealed to be related to differences in intergranular crack propagation mechanisms. The governing crack growth process is in both cases dominated by grain boundary dislocation activities leading to grain boundary sliding. For the thinner specimens, secondary nanocracks are generated (as a result of grain boundary sliding) ahead of the main crack and coalesce together. Instead, secondary nanocracks do not form ahead of the main crack tip.

© 2017 Acta Materialia Inc. Published by Elsevier Ltd. All rights reserved.

#### 1. Introduction

The understanding of plastic deformation mechanisms in nanocrystalline (nc) metals and the related grain size effects has greatly improved over the last twenty years [1–5] but many aspects remain controversial. For example, atomistic simulations can predict a material-dependent grain size below which transgranular dislocation activities become negligible compared to grain boundary (GB) mediated processes [6] while some experiments have confirmed [7] or infirmed [8] such transition for very small grains. In situ experiments can also quantify or identify the respective role of each mechanism in monotonic deformation [9] or even dynamic recovery [10]. In comparison, the mechanisms responsible for cracking in nc metals are not as well understood, due in part to the complications associated with the increased stress field near the crack tip. Atomistic simulations on nc Ni (grain sizes ranging from 5 to 10-12 nm) revealed that the amplified stresses ahead of the crack tip trigger transgranular dislocations that would otherwise not occur in such small grains [11,12]. Artificial or natural stress concentrators such as notches and cracks in

https://doi.org/10.1016/j.actamat.2017.10.004

1359-6454/© 2017 Acta Materialia Inc. Published by Elsevier Ltd. All rights reserved.

free standing nc films also demonstrated stress-assisted grain growth at room temperature [13–15]. This effect was also encountered in larger nc Ni specimen [16]. The large stresses also result in grain boundary decohesion and nano-void formation that may coalesce with the main crack, leading to intergranular fracture (in contrast to the typical transgranular cracking in coarse-grained metals) [11,12]. However, simulations on nc Al (grain size: 5 nm) ahead of a "blunt" crack (or nano-notch, with a root radius of 5 nm) highlighted the role of grain rotation (similar to the Ashby-Verral mechanism [17]) ahead of the notch, which resulted in a homogeneous (gradient free) stress field and led to the conclusion that nc metals may be insensitive to stress concentration [18]. Experimentally, grain rotation near a crack tip in nc Al has been observed at room temperature [19], and then refuted [20]. Explored in a more quantitative way recently, it was found that grain rotation is a mechanism that participates to plastic deformation in nc Al thin films, but is not the main stress-relaxation mechanism [21]. From these studies, stress-assisted grain growth (probably carried out by shear-coupled migration [22-25]) appear as the dominant mechanism of stress relaxation in nc metals [15], while grain rotation only accommodates local grain incompatibilities. Such discrepancies highlight the challenges in capturing the governing mechanisms in nc metals and especially those associated with crack

<sup>\*</sup> Corresponding author. E-mail address: olivier.pierron@me.gatech.edu (O.N. Pierron).

A few experimental studies have been carried out to specifically unveil the crack propagation mechanisms using in situ TEM observations on ultrathin films (<200 nm) [26-35]. These studies may not be representative of bulk nc metals, due to the presence of free surfaces, and other thin film effects such as a lower confinement of the grains [29,36]. Nonetheless, in situ TEM experiments provide a unique opportunity to observe the deformation mechanisms at the crack tip and directly compare them with atomistic simulations, and are relevant for assessing the reliability of ultrathin films used as structural components in micro/nanoelectromechanical systems (MEMS/NEMS) and other emerging applications [37]. Most of these in situ TEM observations revealed intergranular crack growth via nucleation and growth of nanovoids at triple junctions and/or grain boundary nanocracks, and their coalescence to the main crack, as predicted by the simulations of Farkas et al. [11,12], even though the experimental grain sizes are significantly larger (electroplated Ni with average grain size of 30 nm and narrow grain size distribution (unknown thickness) [29], 100-nm-thick pulsed laser deposited Ni with grain size ranging from 5 to 30 nm [27], 125-nm-thick sputter-deposited Al with grains ranging from 35 to 420 nm (average grain size: 130 nm) [26], and 60-nm-thick sputter-deposited Ag with grains ranging from 10 to 120 nm (average grain size: 40 nm) [35]). These studies mainly observed transgranular dislocation activities that led to the coalescence events, sometimes due to necking of the connecting regions. Most studies did not observe GB dislocations or grain rotation in the cracking process [26,27,29]. In the present study, we clearly show that intergranular crack growth mechanisms rely on GB dislocations. We further demonstrate that the GB dislocation mechanisms result in a cracking process that depends on grain and film size, with nanocracks developing favorably ahead of the main crack in thinner films where the average grain size is also smaller.

#### 2. Experimental methods

#### 2.1. Specimen fabrication and characterization

Fig. 1(a) shows the dogbone-shaped Au thin film specimens that were used in this study. The same batch fabrication process was employed to fabricate both types of specimen, the only difference being the thickness of the deposited Au layer. First, high resolution photo-lithography was performed with a negative resist deposited onto a (100) Si substrate. Au films with thicknesses of 30 and 100 nm were deposited using a Denton Ebeam Evaporator with a base pressure of 8  $\times$   $10^{-7}$  Torr and a rate of 0.5 Å/s with 99.99% purity of the target. Then, a lift-off technique was used by acoustic agitation in an acetone solution. Finally, XeF<sub>2</sub> etching of the Si substrate (using a Xactix XeF<sub>2</sub> etcher) was performed to release the specimens from the substrate. As shown in Fig. 1(a), rows of freestanding specimens are connected to large islands of Au that are still anchored to the substrate after the etching, through small tethers that are severed during the manipulation of the specimens onto the MEMS device for testing.

The specimens have a gauge length of  $20 \ \mu m$  and a gauge width of ~1.5  $\mu$ m. The SEM images in Fig. 1 (a) show that the freestanding cantilevers are flat and therefore free from residual stress. The TEM images and their corresponding diffraction patterns in Fig. 1(b)–(e) show that the specimens are nc films with no in-plane texture. Despite having similar fabrication recipes, the thinner films differ significantly in grain size distribution from the thicker films (see Fig. 1(f); grain size distribution calculated from SEM images of the gauge section of the specimens that give reasonable contrast along grain boundaries to measure the diameter of each grain). The 30 nm-thick films have an average grain size  $\overline{d}$  of 40 nm and narrow grain size distribution (see Fig. 1(d) and (e)) compared to 100 nm films, having  $\overline{d} = 70 \text{ nm}$  and range of grains from 10 to 350 nm in diameter (see Fig. 1(b) and (c)). Atomic force microscopy (AFM) was also used to measure the surface roughness of the two films. For each film thickness, three sets of 2 µm by 2 µm AFM scans were measured (see an example in Fig. 1(g) and (h), for 100 and 30 nm thickness respectively), and the surface roughness (rms value) was averaged from the three sets. For 30 nm, the roughness is  $0.52 \pm 0.04$  nm, and for 100 nm, the roughness is  $1.17 \pm 0.43$  nm. The surface roughness is known to increase with increasing deposition rates [38,39], and therefore our roughness values are small given the low deposition rates (0.5 Å/s) used in this study. The deepest measured groove was 2.6 nm for the 30 nm films (8.5% of the film thickness), and 6.2 nm for the 100 nm films (6.2% of the film thickness).

#### 2.2. MEMS nanomechanical testing

#### 2.2.1. Experimental setup

The micron-sized ultrathin specimens were mechanically tested using a microelectromechanical system (MEMS) device shown in Fig. 2(a) and schematized in Fig. 2(b) [40–45]. The device is bulk micromachined using the MEMSCAP SOIMUMPS process. The structural layer is 10 µm thick and is isolated from the wafer by a 1micron-thick oxide layer. It comprises a thermal actuator (providing a displacement  $X_A \sim 1.6 \ \mu m$  (without any specimen) for an input voltage  $V_{in} = 4$  V), a specimen gap, two capacitive sensors located on each side of the specimen gap, and a load sensor. A heat sink, located next to the actuator, help minimizing the temperature increase near the specimen to less than 10 °C [44]. All these components are fabricated over a through-wafer window, thereby allowing TEM imaging. The first capacitive sensor, CS<sub>1</sub>, is rigidly connected to the thermal actuator (i.e. their displacements X are equal,  $X_{CS1} = X_A$ ) using non-conductive epoxy glue which electrically isolates the thermal actuator from the capacitive sensors. The second capacitive sensor, CS<sub>2</sub>, is rigidly connected to the load sensor  $(X_{CS2} = X_{LS})$ , and is identical to  $CS_1$ . The load sensor is made of 4 beams (length: 500 µm) deforming in bending (stiffness, K<sub>LS</sub>, of 100 or 480 N/m depending on the beams width [44]). The specimen gap is ~5 µm, and consists of two adjacent large areas for clamping of the specimen onto the MEMS device. The specimen is clamped to the device using UV curable glue, as shown in Fig. 2(d), and a micromanipulator (see details in Refs. [40–42]).

A test consists of applying a displacement  $X_A$  by controlling  $V_{in}$ , resulting in the elongation of the specimen ( $X_S$ ) and the displacement of the load sensor ( $X_{LS}$ ). The applied force is given by:

$$F = K_{LS} * X_{LS} = K_{LS} * X_{CS2} \tag{1}$$

while the elongation of the specimen,  $X_S$ , is obtained via the difference between the displacement of the two capacitive sensors:

$$X_{\rm S} = X_{\rm A} - X_{\rm LS} = X_{\rm CS1} - X_{\rm CS2} \tag{2}$$

The applied stress is obtained by dividing F by the specimen's cross sectional area, and the strain by dividing  $X_S$  by the specimen's gauge length.

#### 2.2.2. Ex situ tests

The tensile stress-strain curve were obtained for both types of specimens by performing ex situ tests. The change in capacitance of sensors  $CS_1$  and  $CS_2$ ,  $\Delta CS_1$  and  $\Delta CS_2$ , were independently measured

Download English Version:

## https://daneshyari.com/en/article/5435683

Download Persian Version:

https://daneshyari.com/article/5435683

Daneshyari.com